Experience-Dependent Equilibration of AMPAR-Mediated Synaptic Transmission during the Critical Period

Citation: Han, Kyung-Seok, Samuel F. Cooke, and Weifeng Xu. "Experience-Dependent Equilibration of AMPAR-Mediated Synaptic Transmission during the Critical Period." Cell Reports 18.4 (2017): 892–904.

As Published: http://dx.doi.org/10.1016/j.celrep.2016.12.084

Publisher: Elsevier

Persistent URL: http://hdl.handle.net/1721.1/110049

Version: Final published version: final published article, as it appeared in a journal, conference proceedings, or other formally published context

Article

Cell Reports

Experience-Dependent Equilibration of AMPAR-Mediated Synaptic Transmission during the Critical Period

Graphical Abstract

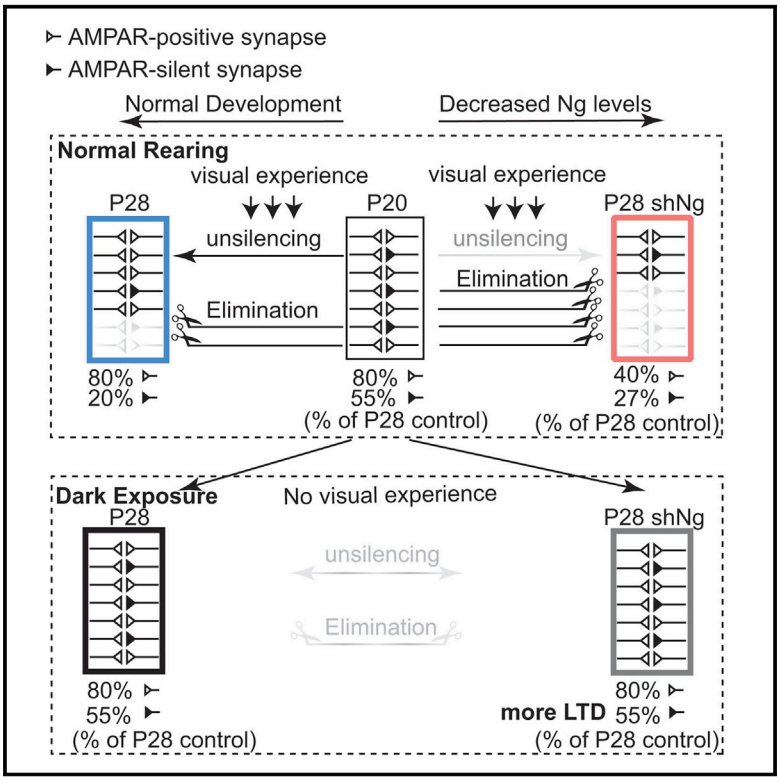

Highlights

- AMPAR-mediated synaptic transmission remains at equilibrium during the critical period
- Ng is required for the maintenance of AMPAR-mediated synaptic transmission
- AMPAR-silent synapse conversion and synapse elimination equilibrate synaptic responses
- Ng coordinates these two experience-dependent processes for circuit optimization

Authors

Kyung-Seok Han, Samuel F. Cooke, Weifeng Xu

Correspondence

weifeng@mit.edu

In Brief

Han et al. find that experience-dependent elimination of glutamatergic synapses and conversion of AMPAR-silent synapses to AMPAR-positive synapses together maintain AMPAR-positive synapses at equilibrium during the critical period. Neurogranin coordinates these processes for functional optimization and experience-dependent maturation of excitatory circuits.

Han et al., 2017, Cell Reports *18*, 892–904
January 24, 2017
http://dx.doi.org/10.1016/j.celrep.2016.12.084

OPEN ACCESS
CellPress

Cell Reports
Article

Experience-Dependent Equilibration of AMPAR-Mediated Synaptic Transmission during the Critical Period

Kyung-Seok Han,[1] Samuel F. Cooke,[1,2] and Weifeng Xu[1,3,*]
[1]Picower Institute for Learning and Memory, Department of Brain and Cognitive Sciences, Massachusetts Institute of Technology, Cambridge, MA 02139, USA
[2]Present address: Maurice Wohl Institute for Clinical Neuroscience, Department of Basic and Clinical Neuroscience, Institute of Psychiatry, Psychology and Neuroscience, King's College London, London SE5 9RT, UK
[3]Lead Contact
*Correspondence: weifeng@mit.edu
http://dx.doi.org/10.1016/j.celrep.2016.12.084

SUMMARY

Experience-dependent synapse refinement is essential for functional optimization of neural circuits. However, how sensory experience sculpts excitatory synaptic transmission is poorly understood. Here, we show that despite substantial remodeling of synaptic connectivity, AMPAR-mediated synaptic transmission remains at equilibrium during the critical period in the mouse primary visual cortex. The maintenance of this equilibrium requires neurogranin (Ng), a postsynaptic calmodulin-binding protein important for synaptic plasticity. With normal visual experience, loss of Ng decreased AMPAR-positive synapse numbers, prevented AMPAR-silent synapse maturation, and increased spine elimination. Importantly, visual deprivation halted synapse loss caused by loss of Ng, revealing that Ng coordinates experience-dependent AMPAR-silent synapse conversion to AMPAR-active synapses and synapse elimination. Loss of Ng also led to sensitized long-term synaptic depression (LTD) and impaired visually guided behavior. Our synaptic interrogation reveals that experience-dependent coordination of AMPAR-silent synapse conversion and synapse elimination hinges upon Ng-dependent mechanisms for constructive synaptic refinement during the critical period.

INTRODUCTION

Postnatal refinement of existing neural circuits through experience occurs during a period of heightened glutamatergic synaptic plasticity (Fagiolini et al., 1994; Kirkwood et al., 1995), commonly described as the critical period. Experience-dependent establishment and strengthening of functional connections during the critical period are thought to play an essential role in the formation of fully functional neural circuits during postnatal development (Ashby and Isaac, 2011; Ishikawa et al., 2014; Wu et al., 1996). On the other hand, anatomical studies have revealed that pruning of existing connections during the critical period also contributes to the refinement of neural circuits (Antonini and Stryker, 1993; Holtmaat et al., 2005; Zuo et al., 2005a). These two seemingly antagonistic processes for modifying connectivity allow experience to sculpt excitatory neural circuits during development. How these processes are coordinated to produce functional optimization is poorly understood.

Fast, excitatory synaptic transmission in the mammalian central nervous system is primarily mediated by two types of ionotropic glutamatergic receptors, α-amino-3-hydroxy-5-methyl-4-isoxazolepropionic acid receptors (AMPARs) and *N*-methyl-D-aspartate receptors (NMDARs). Although all glutamatergic synapses contain NMDARs, they are sub-categorized into two major types: AMPAR-positive and AMPAR-silent synapses, also defined as active and silent synapses (Liao et al., 1995). The recruitment of AMPARs to AMPAR-silent synapses (unsilencing) and the stabilization of the unsilenced synapses, the process that converts AMPAR-silent synapses to AMPAR-positive synapses, is thought to be important for glutamatergic synapse maturation (Huang et al., 2015) and the strengthening of neural connectivity during postnatal development (Ashby and Isaac, 2011; Wu et al., 1996). Functional analyses point toward an NMDAR-dependent mechanism akin to long-term potentiation (LTP) that unsilences AMPAR-silent synapses (Isaac et al., 1995; Liao et al., 1995; Rumpel et al., 1998). Were it to act alone or even predominate, this mechanism would enhance glutamatergic synaptic transmission, consistent with observed increases in the number of AMPAR-positive synapses at certain developmental stages (Ashby and Isaac, 2011; Phillips et al., 2011).

It has also been shown that axon arbors, the presynaptic structural correlate, and dendritic spines, the postsynaptic structural correlate of excitatory synapses, are eliminated during postnatal development as neural circuits are refined (Antonini and Stryker, 1993; Holtmaat et al., 2005; Zuo et al., 2005a), suggesting a loss of connectivity at the anatomical level. Sensory deprivation prevents spine elimination, and recovery from sensory deprivation and heightened sensory experience leads to accelerated spine elimination, suggesting that synapse elimination during development requires experience (Bian et al., 2015;

Zuo et al., 2005b). Although it has been proposed that spine elimination and stabilization are coordinated events during development (Bian et al., 2015), the functional impact of experience-dependent refinement on glutamatergic synaptic transmission is unknown.

Calcium entry through postsynaptic NMDARs activates intracellular signaling cascades including Ca^{2+}/calmodulin (CaM)-dependent protein kinase II (CaMKII) and calcineurin. The spatiotemporal abundance of this Ca^{2+}/CaM complex determines the direction of synaptic plasticity, resulting in LTP (Malinow et al., 1988; Meyer et al., 1992; Silva et al., 1992) or long-term depression (LTD) (Mulkey et al., 1994; Torii et al., 1995; Zeng et al., 2001). CaMKII activation mimics experience-dependent conversion of AMPAR-silent synapses to AMPAR-positive synapses in the central nervous system of *Xenopus* (Wu et al., 1996) and is required for experience-dependent plasticity in the neocortex (Glazewski et al., 1996; Taha et al., 2002). Conversely, NMDAR-dependent LTD requires activation of calcineurin (Mulkey et al., 1994) and is associated with shrinkage or loss of synapses (Becker et al., 2008; Wiegert and Oertner, 2013; Zhou et al., 2004). These findings led us to hypothesize that the Ca^{2+}/CaM-mediated signaling cascades balance experience-dependent synapse maturation and elimination.

It is known that CaM concentrations remain relatively constant in neurons (Baimbridge et al., 1992). However, a family of proteins can regulate its availability and thus the Ca^{2+}/CaM dynamics (Slemmon et al., 2000). Among those proteins, neurogranin (Ng) is enriched in the hippocampus and cerebral cortex, primarily in the postsynaptic compartment of principal neurons (Higo et al., 2004; Represa et al., 1990; Singec et al., 2004; Watson et al., 1992). It is believed that Ng preferentially binds to apo-CaM and suppresses the formation of Ca^{2+}-saturated Ca/CaM (Gaertner et al., 2004). Given that Ng is more abundant than CaM in the postsynaptic compartment, in neurons under a resting condition with cytosolic Ca^{2+} levels ranging from 50 nM to a few μM, it is predicted that the majority of CaM is bound to Ng and, upon elevation of Ca^{2+} levels, Ng dissociates from CaM to reveal a pool of CaM to the Ca^{2+} influx (Zhabotinsky et al., 2006). This suggests that Ng may regulate dendritic Ca^{2+}/CaM-dependent signaling (Petersen and Gerges, 2015) and influence experience-dependent plasticity of cortical circuitry. Ng starts to express postnatally and its expression ramps up during development (postnatal day [P]3–P30) in rodents (Represa et al., 1990) and non-human primates (Higo et al., 2004). Levels of Ng in the hippocampus are positively correlated with hippocampus-dependent learning performance (Huang et al., 2004). Loss of Ng in mice causes an impairment of spatial learning, in addition to altering synaptic plasticity in the hippocampus (Pak et al., 2000), whereas increasing Ng levels in the prefrontal cortex facilitates memory extinction and synaptic plasticity at prefrontal glutamatergic synapses (Zhong et al., 2015). Together, these findings suggest an important role of Ng in regulating synaptic plasticity in the central nervous system.

The Ng gene has been associated with schizophrenia (SCZ) (Ruano et al., 2008; Stefansson et al., 2009) and a rare genetic intellectual disability (ID) disorder known as Jacobsen syndrome (Coldren et al., 2009), suggesting dysfunction of Ng-dependent pathways in the pathophysiology of SCZ and ID. Interestingly, heightened synapse elimination during postnatal development has been recently suggested to play an essential role in the etiology of schizophrenia (Sekar et al., 2016). However, little is known about how Ng might be involved in synapse elimination.

Here we analyze the developmental profile of glutamatergic transmission during the critical period using the mouse primary visual cortex as the model system. By manipulating Ng, we investigate how Ca^{2+}/CaM-mediated signaling controls experience-dependent developmental progression of excitatory synaptic connectivity in the primary visual cortex during this time window.

RESULTS

AMPAR-Mediated Synaptic Transmission Is Maintained at Equilibrium while Glutamatergic Synapses Mature during the Critical Period

To estimate AMPAR-mediated synaptic transmission, we recorded AMPAR miniature excitatory synaptic currents (mEPSCs). This approach provides measurements of the frequency and unitary strength of AMPAR-positive synapses. We first examined AMPAR mEPSCs at layer (L)2/3 pyramidal neurons between P20 and P28, the beginning and height, respectively, of the critical period in mouse primary visual cortex (V1) (Figure 1A). Both the averaged frequency and amplitude of mEPSCs were similar between P20 and P28 mice (Figures 1B and 1C; individual data points in this and subsequent figures were replotted according to animals in the corresponding supplemental figures), indicating that the strength of overall AMPAR-mediated synaptic input was maintained at similar levels between P20 and P28.

We then characterized the ratio of AMPAR- and NMDAR-mediated synaptic currents (AMPAR/NMDAR ratio) at visual cortical L4 to L2/3 synapses at P20 and P28. We found that the AMPAR/NMDAR ratio was significantly higher in P28 mice compared to P20 mice (Figure 1D). The increase of the AMPAR/NMDAR ratio indicates a decrease in the proportion of AMPAR-silent synapses. To directly measure the level of AMPAR-silent synapses at visual cortical L4–L2/3 synapses, we used minimal stimulation to perform failure analysis to extract the relative proportion of AMPAR-silent synapses at P20 and P28 (Liao et al., 1995). Consistent with previous studies (Huang et al., 2015), we found that the proportion of AMPAR-silent synapses was significantly lower in P28 mice compared to P20 mice (Figures 1E and 1F), indicating that the proportion of AMPAR-silent synapses of the overall glutamatergic synapse population decreases during visual cortical development. This is consistent with the idea that AMPAR-silent synapses mature during the critical period, illustrated by the decrease in the proportion of synapses that are AMPAR-silent (Huang et al., 2015).

Thus far, we have found that from P20 to P28, AMPAR-positive synaptic responses remain stable, whereas the proportion of AMPAR-silent synapses decreases. To assess changes in glutamatergic synaptic connectivity, we analyzed our electrophysiology data and estimated the fractions of AMPAR-positive and AMPAR-silent synaptic responses at P20 normalized to the control conditions in P28 mice. The calculation (see Supplemental Experimental Procedures) revealed that between P20 and P28, AMPAR-mediated synaptic responses are maintained

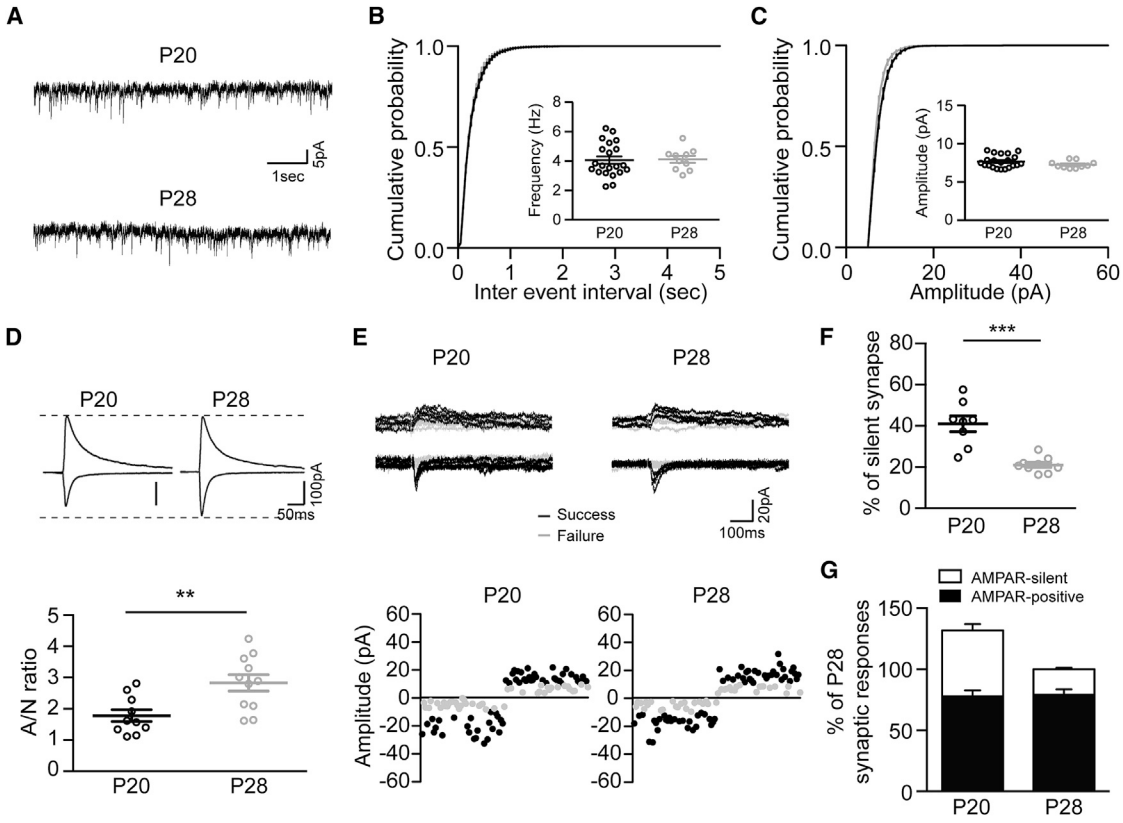

Figure 1. Equilibrium of AMPAR-Mediated Synaptic Transmission during the Critical Period

(A) Representative traces for AMPAR-mediated mEPSCs recorded at visual cortical L2/3 neurons from P20 and P28 mice.

(B) Cumulative probability plots of AMPAR mEPSC inter-event intervals from P20 (black) and P28 (gray). Inset bar graph showing averaged mEPSC frequency (Hz): P20, n = 21 neurons/6 mice, 4.06 ± 0.25; P28, n = 10/4, 4.12 ± 0.24. Here and thereafter, unless indicated otherwise, each data point of frequency is presented as a circle, and mean ± SEM is plotted. Student's t test was used for two-sample datasets unless indicated otherwise; p = 0.881.

(C) Cumulative probability plots of AMPAR mEPSC amplitude from P20 and P28. Inset bar graph showing averaged mEPSC amplitude (pA): P20, n = 21 neurons/6 mice, 7.67 ± 0.18; P28, n = 10/4, 7.26 ± 0.15. In this panel and thereafter unless indicated otherwise, each data point of amplitude is presented with a circle, and mean ± SEM is plotted; Student's t test was used for two-sample datasets unless indicated otherwise, p = 0.160.

(D) Representative traces of EPSCs recorded at holding voltage potential (V_h) = −70 mV and V_h = +40 mV in L4–L2/3 synapses from P20 and P28 mice. Summary graph of the AMPAR/NMDAR EPSC ratio. P20, n = 10 slices/4 mice, 1.78 ± 0.19; P28, n = 11/4, 2.83 ± 0.26. In this panel and thereafter unless indicated otherwise, each data point of A/N ratio is presented with a circle, and mean ± SEM is plotted; Student's t test was used for two-sample datasets unless indicated otherwise, **p < 0.01.

(E) Representative traces of EPSCs recorded at V_h = −70 mV and V_h = +40 mV with minimal stimulation from P20 and P28. Success responses are marked in black, whereas failure responses are marked in gray. Amplitude of success (black) and failure (gray) of EPSCs by minimal stimulation from P20 and P28 mice.

(F) Summary graph of % AMPAR-silent synapses. P20 (open black), n = 8 slices/5 mice, 40.99% ± 3.85%; P28 (open gray), n = 9/4, 20.99% ± 1.23%. In this panel and thereafter unless indicated otherwise, each data point of percent AMPAR-silent synapse is presented with a circle, and mean ± SEM is plotted; Student's t test was used for two-sample datasets unless indicated otherwise, ***p < 0.001.

(G) Summary bar graph showing % of AMPAR-positive synapses (black) and AMPAR-silent synapses (white) in L2/3 pyramidal neurons in V1 from P20 and P28 mice, normalized to the condition at P28.

at a similar level but the number of AMPAR-silent synapses differs (Figure 1G): at P20, there is a higher overall glutamatergic synaptic connectivity compared to that at P28 (Figure 1G; ~140% of P28 synaptic responses) due to sustained AMPAR-positive synaptic responses and a higher proportion of AMPAR-silent synapses.

Ng Is Required to Maintain Basal AMPAR-Positive Synapses

We hypothesized that during the critical period, experience-dependent processes hinge upon Ca^{2+}/CaM-dependent signaling pathways to sculpt excitatory synaptic transmission. To tap into this experience-dependent process, we targeted Ng, which is expressed exclusively in glutamatergic excitatory neurons in the cortex (Singec et al., 2004), and sought to regulate Ca^{2+}-dependent signaling critical for NMDAR-dependent synaptic plasticity at glutamatergic synapses (Zhabotinsky et al., 2006). To verify the expression profile of Ng in the primary visual cortex, we dissected the V1 region from mouse brains at different ages and measured the Ng protein level in the lysate using western blots in comparison to CaMKIIα and CaM (Figures 2A and 2B). As expected, Ng showed a postnatal onset of expression, and the

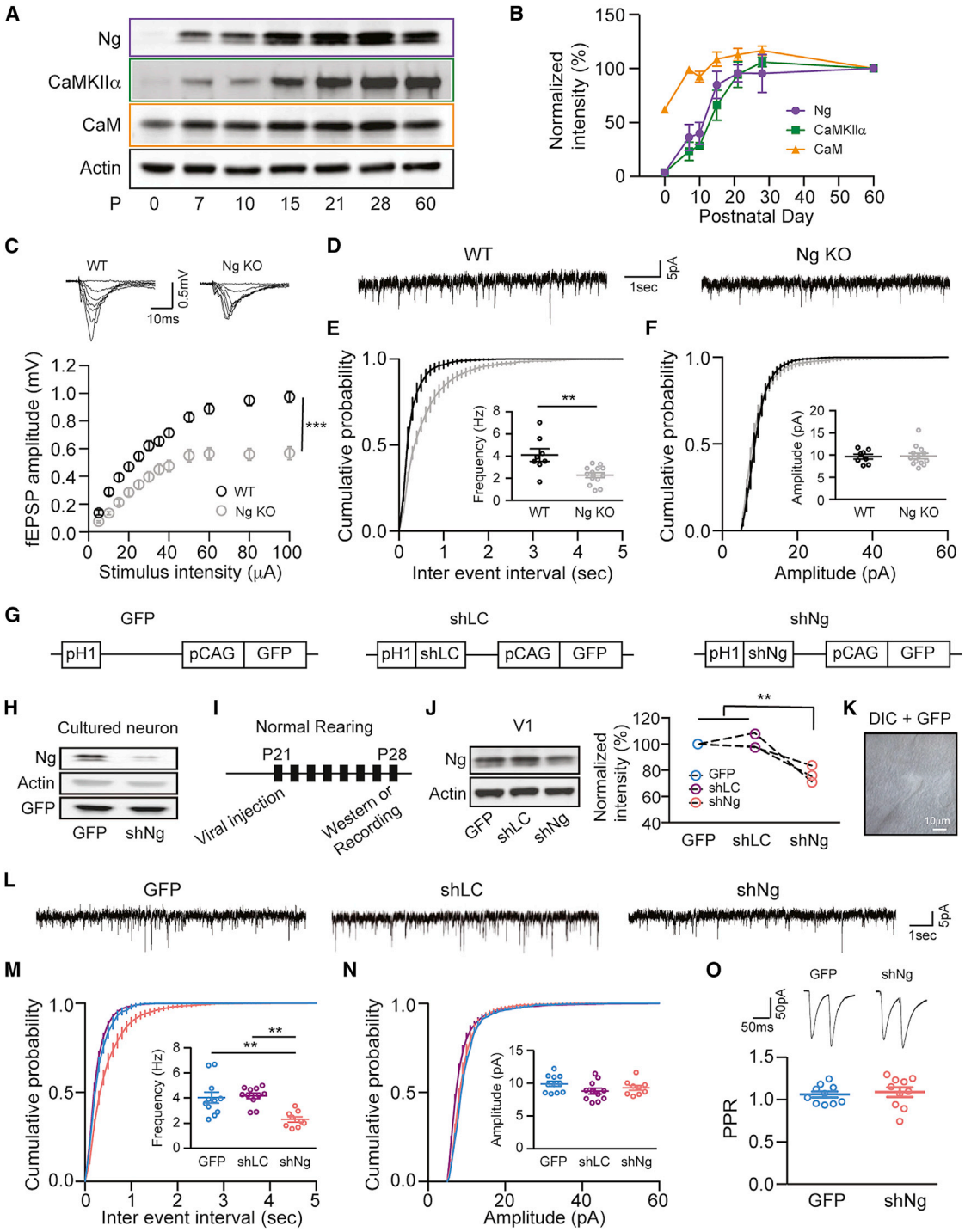

Figure 2. Decrease of Ng Reduced Basal Synaptic Transmission and the Frequency of mEPSCs

(A) Example western blot images of neurogranin (Ng; purple box), CaMKIIα (green box), and calmodulin (CaM; orange box) from the primary visual cortical lysate during development.

(B) Relative intensity of Ng (purple), CaMKIIα (green), and CaM (orange) protein levels during development, normalized to the protein levels at P60. Protein loading was normalized to actin intensity. Symbols are mean ± SEM.

(C) Sample traces (upper) and input-output curve (lower) for basal synaptic transmission in L4–L2/3 synapses of the primary visual cortex from WT (open black) and Ng KO (open gray) mice. At the maximum stimulation intensity, WT, n = 10 slices/3 mice, 0.97 ± 0.04 mV; Ng KO, n = 13/3, 0.57 ± 0.05 mV. Symbols are means ± SEM, Student's t test, ***$p < 0.0001$.

(D) Sample traces for AMPAR-mediated mEPSCs recorded at visual cortical L2/3 neurons in WT and Ng KO mice.

(legend continued on next page)

expression ramped up during development, reaching a plateau after the critical period (Figure 2B). The expression profile of Ng is similar to that of CaMKIIα, a well-known player essential for synaptic plasticity, whereas CaM, the interaction partner of Ng, was already expressed at a relatively high level at P0, and reached the plateau at an earlier developmental stage (P10). This result shows that an increase in Ng expression coincides with the developmental window of experience-dependent synaptic plasticity in the primary visual cortex, suggesting a functional role of Ng in this process.

If Ng is involved in experience-dependent refinement of the primary visual cortex, we expected that excitatory synaptic transmission in V1 would be affected in mice with Ng deletion. We measured the field excitatory postsynaptic potential (fEPSP) from L4–L2/3 synapses in Ng knockout (Ng KO) mice (Pak et al., 2000) and their wild-type (WT) littermates at P28–P30. The average fEPSP amplitudes at all stimulus levels in Ng KO mice were at ~50% of the level of those in WT littermates (Figure 2C), showing a decreased excitatory synaptic strength with Ng deletion correlated with a decrease in visually evoked potential magnitude recorded in vivo in Ng KO mice (data not shown). We then measured AMPAR mEPSCs in L2/3 pyramidal neurons from Ng KO mice and WT littermates (Figure 2D). Interestingly, Ng KO mice showed a significant decrease in mEPSC frequency relative to WT littermate controls (Figure 2E) without affecting the mean amplitude of mEPSCs (Figure 2F). These results demonstrate that loss of Ng causes significantly weaker basal glutamatergic synaptic transmission in V1, associated with a decreased frequency of synaptic events.

To test whether the deficit seen in the Ng KO mice is due to a decrease of Ng in V1, we locally knocked down the expression of Ng in V1 using an adeno-associated virus (AAV) expressing an shRNA to target Ng expression (shNg; Figure 2G). An AAV containing the H1 promoter and CAG-driven GFP expression (GFP) and an AAV expressing an shRNA that targeted luciferase expression (shLc) were used as the virus-infection controls (Figure 2G). Using cultured cortical neurons to test the efficacy of the viral approach, we found that shNg significantly reduced the expression levels of Ng in neurons transduced with shNg AAV, compared to the levels of Ng in neurons transduced with GFP AAV (Figure 2H). We then injected GFP-AAV, shLc-AAV, and shNg-AAV into V1 of P21 mice and then punched GFP-expressing V1 tissue at P28 (Figure 2I) to perform a western blot assay on the lysate. The endogenous Ng levels in V1 were significantly decreased in shNg-AAV-infected samples, compared to GFP-AAV- and shLc-AAV-infected samples (Figure 2J). We next recorded mEPSCs from transduced pyramidal neurons in L2/3 at P28 (Figures 2K and 2L). Consistent with the results from the Ng knockout mice, the frequency of mEPSCs was reduced by ~50% in the shNg-transduced neurons compared to those of GFP- and shLc-transduced control neurons (Figure 2M). In contrast, the average amplitudes of mEPSCs were not significantly different between shNg-transduced and control neurons (Figure 2N). Therefore, decreasing Ng in V1 caused a decrease in AMPAR-mediated synaptic transmission, demonstrating that normal expression of Ng in V1 between P21 and P28 is critical for maintaining AMPAR-mediated synaptic transmission.

A change in mEPSC frequency could be caused by altering either presynaptic release probability or the total number of AMPAR-positive synapses. Therefore, we tested whether loss of Ng affects presynaptic release probability by measuring the paired pulse ratio (PPR) at L4–L2/3 synapses, which is roughly inversely correlated with the release probability. The PPRs were not significantly different between shNg-transduced neurons and GFP-transduced neurons (Figure 2O), indicating that decreased expression of Ng in V1 had little impact on presynaptic release probability at L4–L2/3 synapses. Thus, lowered mEPSC frequency by shNg in L2/3 pyramidal neurons likely results from a reduction in the number of AMPAR-positive synapses. Overall, these findings show that Ng is required to maintain AMPAR-positive synapse numbers during the critical period.

Visual Experience Is Required for the Deficits in Glutamatergic Transmission in V1 Resulting from Decreased Ng

Given that visual experience plays an essential role in sculpting circuits during the critical period, we hypothesized that synaptic

(E) Cumulative probability plots of AMPAR mEPSC inter-event intervals in WT (black) and Ng KO (gray) mice. Averaged mEPSC frequency (Hz): WT, n = 8 neurons/3 mice, 4.10 ± 0.48; Ng KO, n = 13/3, 2.28 ± 0.21. **p < 0.01.
(F) Cumulative probability plots of AMPAR mEPSC amplitude in WT (black) and Ng KO (gray) mice. Averaged mEPSC amplitude (pA): WT, n = 8 neurons/3 mice, 9.65 ± 0.47; Ng KO, n = 13/3, 9.79 ± 0.58. p = 0.87.
(G) Bicistronic AAV constructs, one encoding GFP control (GFP) and one encoding GFP and shRNA targeting luciferase (shLC) and Ng (shNg).
(H) Representative images of western blots for Ng, actin, and GFP in cortical neuron cultures transduced with GFP-AAV and shNg-AAV.
(I) Timeline of viral injection and experiments.
(J) Representative images and normalized intensity of western blots for Ng and actin in the primary visual cortex (from three mice) transduced with GFP-AAV (open blue), shLC-AAV (open purple), and shNg-AAV (open light red). One-way ANOVA, Bonferroni's multiple comparisons test; **p < 0.01.
(K) An L2/3 pyramidal neuron transduced with shNg in the visual cortex.
(L) Sample traces for AMPAR-mediated mEPSCs recorded at visual cortical L2/3 neurons from GFP-AAV-, shLC-AAV-, and shNg-AAV-transduced neurons.
(M) Cumulative probability plots of AMPAR mEPSC inter-event intervals in GFP-AAV- (blue), shLC-AAV- (purple), and shNg-AAV-transduced (light red) neurons. Averaged mEPSC frequency (Hz): GFP, n = 10 neurons/4 mice, 4.03 ± 0.44; shLC, n = 11/3, 4.17 ± 0.22; shNg, n = 9/3, 2.30 ± 0.20. One-way ANOVA, Tukey's multiple comparisons test; **p < 0.01.
(N) Cumulative probability plots of AMPAR mEPSC amplitude in GFP-AAV- (blue), shLC-AAV- (purple), and shNg-AAV-transduced (light red) neurons. Averaged mEPSC amplitude (pA): GFP, n = 10 neurons/4 mice, 10.11 ± 0.39; shLC, n = 11/3, 8.79 ± 0.44; shNg, n = 9/3, 9.31 ± 0.36. One-way ANOVA.
(O) The paired pulse ratio (PPR) of 50-ms inter-stimulus intervals in visual cortical L4–L2/3 synapses from GFP-AAV- (open blue) and shNg-AAV-transduced (open light red) neurons. GFP, n = 10 slices/3 mice, 1.08 ± 0.06; shNg, n = 11/3, 1.10 ± 0.05; each data point of PPR is presented with a circle, and mean ± SEM is plotted, Student's t test, p = 0.676.

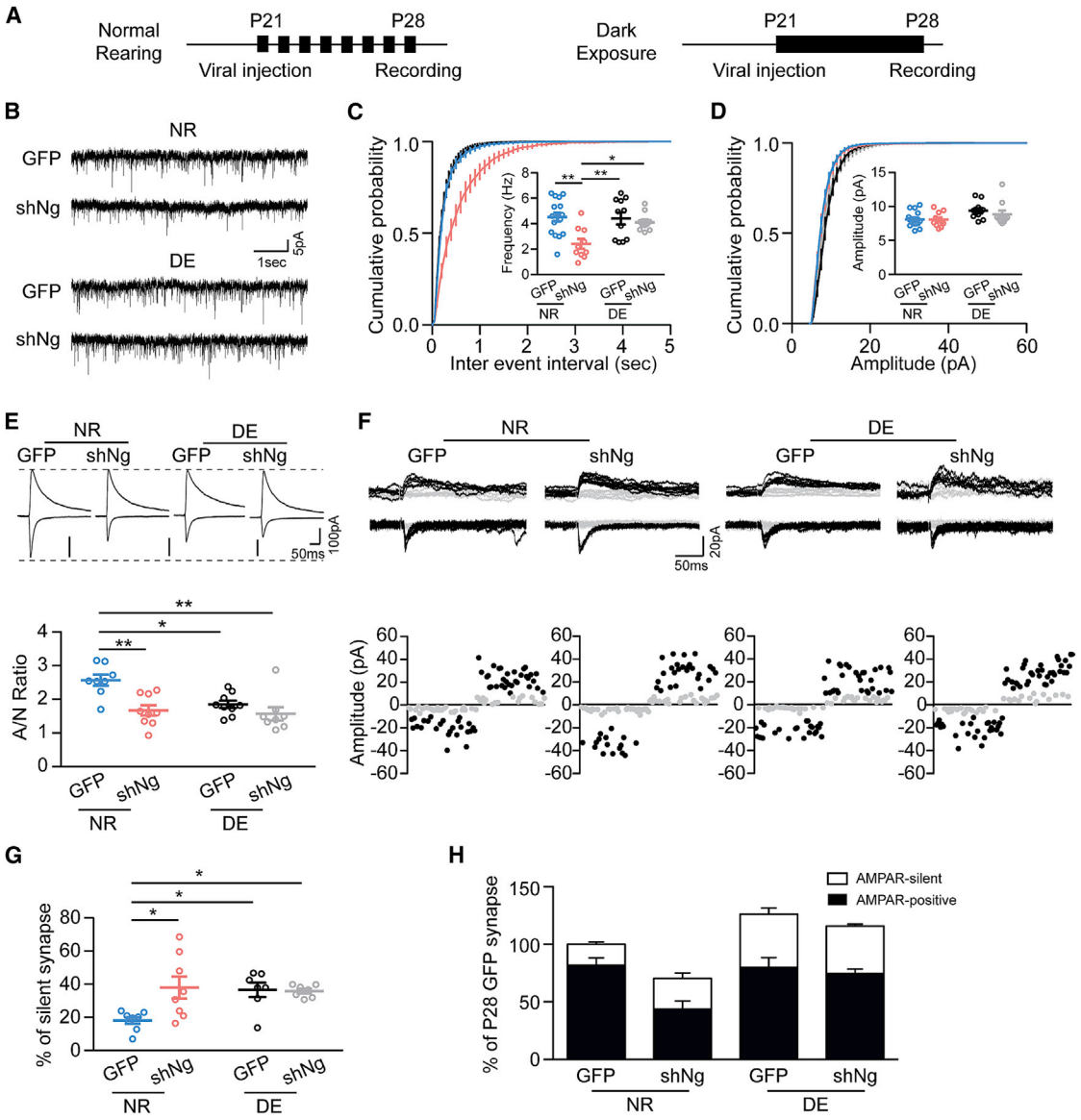

Figure 3. Ng Knockdown Reduced the Number of AMPAR-Positive Synapses and Prevented Developmental Decrease of AMPAR-Silent Synapse Proportion in a Visual-Experience-Dependent Manner

(A) Diagrams of normal rearing (NR) and dark exposure (DE) (from P21 to P28) conditions. The recording is done 1 week after viral injection. Black bars represent darkness.

(B) Sample traces for AMPAR-mediated mEPSCs recorded at visual cortical L2/3 neurons from GFP-AAV- (GFP) and shNg-AAV- (shNg) transduced neurons in NR and DE conditions.

(C) Cumulative probability plots of AMPAR mEPSC inter-event intervals from GFP (blue) and shNg (light red) neurons in NR and GFP (open black) and shNg (gray) neurons in DE. Averaged mEPSC frequency (Hz): GFP NR, n = 16 neurons/5 mice, 4.51 ± 0.35; shNg NR, n = 10/4, 2.41 ± 0.38; GFP DE, n = 11/4, 4.40 ± 0.47; shNg DE, n = 10/5, 4.10 ± 0.23. A two-factor dataset is shown in this panel and thereafter, unless indicated otherwise. Two-way ANOVA, Tukey's multiple comparisons test; *$p < 0.05$, **$p < 0.01$.

(D) Cumulative probability plots of AMPAR mEPSC amplitude in each condition. Averaged mEPSC frequency (pA): GFP NR, n = 16 neurons/5 mice, 8.11 ± 0.28; shNg NR, n = 10/4, 8.05 ± 0.35; GFP DE, n = 11/4, 9.38 ± 0.37; shNg DE, n = 10/5, 8.84 ± 0.56.

(E) Representative traces of EPSCs recorded at $V_h = -70$ mV and $V_h = +40$ mV in L4–L2/3 synapses from GFP-AAV- and shNg-AAV-transduced neurons in NR and DE conditions. Traces are normalized to EPSCs recorded at $V_h = +40$ mV. Summary graph of the AMPAR EPSC/NMDAR EPSC (A/N) ratio. GFP NR, n = 8 slices/4 mice, 2.57 ± 0.17; shNg NR, n = 9/3, 1.67 ± 0.15; GFP DE, n = 9/3, 1.85 ± 0.11; shNg DE, n = 9/3, 1.57 ± 0.20, two-way ANOVA, Tukey's multiple comparisons test, *$p < 0.05$, **$p < 0.01$.

(F) Representative traces of EPSCs recorded at $V_h = -70$ mV and $V_h = +40$ mV with minimal stimulation in L4–L2/3 synapses from virally injected NR and DE mice. The amplitude of success (black) and failure (gray) of EPSCs by minimal stimulation is shown.

(legend continued on next page)

deficits caused by shNg require visual experience. To test this, we eliminated visual input by rearing mice in complete darkness after virus infusion at P21 to deprive them of visual experience during the period of shNg expression (Figure 3A). We then examined glutamatergic synaptic transmission in L2/3 principal neurons in these mice at P28, measuring AMPAR-mediated mEPSCs from transduced pyramidal neurons in normally reared (NR) and dark-exposed (DE) groups (Figure 3B). Recordings were performed in parallel NR and DE groups on alternating days. In the NR group, the frequency of mEPSCs was significantly reduced in shNg-AAV-transduced neurons compared to GFP-AAV-transduced neurons (Figure 3C), whereas in the DE group, the frequencies of mEPSCs were not significantly different between shNg-AAV- and GFP-AAV-transduced neurons (Figure 3C). The averaged amplitudes of mEPSCs did not differ significantly between shNg-AAV- and GFP-AAV-transduced neurons in either the NR or DE groups (Figure 3D). These results reveal that during the critical period, the number of AMPAR-positive synapses in L2/3 pyramidal neurons remains at equilibrium. The maintenance of this equilibrium likely requires experience-induced Ca/CaM-dependent signaling, because decreasing Ng levels led to a loss of AMPAR-positive synapses, potentially by perturbing the Ca/CaM dynamics, and this loss can be prevented by experience deprivation. Thus, Ng is required to maintain visual experience-dependent equilibrium of AMPAR-positive synapses in L2/3 principal neurons during the critical period.

Decrease of Ng Causes Delayed Experience-Dependent AMPAR-Silent Synapse Maturation and Exacerbated Synapse Loss

During the critical period, glutamatergic synapses undergo experience-dependent maturation, characterized by an increase in the AMPAR/NMDAR ratio and a decrease in the proportion of AMPAR-silent synapses (Figures 1D–1F; Huang et al., 2015). Given that decreased Ng levels during the critical period led to an experience-dependent loss of AMPAR-positive synapse numbers, we tested whether decreasing Ng levels affects AMPAR/NMDAR ratios and the proportion of AMPAR-silent synapses.

We measured the AMPAR/NMDAR ratio from GFP-AAV- and shNg-AAV-transduced neurons with the same experimental timeline for minianalysis (shown in Figure 3A). The AMPAR/NMDAR ratio was significantly lower in shNg-AAV-transduced neurons at L4–L2/3 synapses compared to GFP-AAV-transduced neurons in the NR group (Figure 3E). These results suggest that decreasing Ng prevents a developmental increase in the AMPAR/NMDAR ratio. With DE mice after the viral injection at P21, the AMPAR/NMDAR ratios were not significantly different between shNg-AAV- and GFP-AAV-transduced neurons (Figure 3E). The AMPAR/NMDAR ratio in the DE group was significantly lower than in control neurons in the NR group and at a similar level to that in P20 mice. Therefore, both deprivation of experience and loss of Ng prevented the developmental increase of the AMPAR/NMDAR ratio. These results reveal that the developmental increase in the AMPAR/NMDAR ratio depends on experience and requires Ng.

We next measured the proportion of AMPAR-silent synapses with Ng manipulation and visual experience using minimum stimulation and failure analysis. The proportion of AMPAR-silent synapses was higher in shNg-AAV-transduced neurons compared to GFP-AAV-transduced neurons in NR mice (Figures 3F and 3G), suggesting that the decrease in Ng protein levels prevents the developmental maturation of AMPAR-silent synapses. However, in DE mice, the proportion of AMPAR-silent synapses was not significantly different between shNg-AAV- and GFP-AAV-transduced neurons (Figures 3F and 3G). In fact, the proportion of silent synapses was higher in both GFP-AAV- and shNg-AAV-transduced neurons in DE mice compared to that in GFP-AAV-transduced neurons in NR mice (Figure 3G), and was at a similar level to the proportion of silent synapses in P20 mice (Figure 1F). This result is consistent with previous studies showing that deprivation of experience arrests AMPAR-silent synapses at an early developmental level (Ashby and Isaac, 2011; Funahashi et al., 2013). Importantly, this result shows that AMPAR-silent synapse maturation depends on experience and requires Ng.

Thus far, we found that from P20 to P28, the number of AMPAR-positive synaptic responses remains equilibrated (Figure 1B) and the proportion of AMPAR-silent synapses decreases during the critical period (Figure 1F). Ng KD led to a lower number of AMPAR-positive synaptic responses (Figure 2M) and a higher fraction of silent synapses via interaction with visual experience (Figure 3G). Our data predict a net decrease in total excitatory synaptic connections, within which the proportion of AMPAR-silent synapses remained high (Figure 3H). Given the decrease in the number of AMPAR-positive synapses and no further increase in the proportion of AMPAR-silent synapses with Ng KD, our functional data imply that both AMPAR-positive and AMPAR-silent synapses are eliminated. Furthermore, depriving visual experience led to a higher fraction of AMPAR-silent synapses and a sustained number of AMPAR-positive synapses in control neurons compared to the NR condition. This predicts a higher number of synaptic connections in the control neurons in the DE group compared to those in the NR group at P28 (Figure 3H). Judging by the estimated numbers, our results suggest that DE prevents the loss of AMPAR-silent synapses during development and arrests the synaptic connectivity at the earlier developmental stage prior to experience deprivation. In addition, depriving visual experience protects neurons from loss of synaptic connectivity induced by Ng KD. Overall, these results show that Ng is required for experience-dependent maintenance of AMPAR-positive synapses, a process balanced by the loss of AMPAR-positive synapses and conversion of AMPAR-silent synapses to AMPAR-positive synapses. Furthermore, the interaction

(G) Summary graph of % AMPAR-silent synapses. GFP NR, n = 8 neurons/4 mice, 18.09% ± 2.01%; shNg NR, n = 8/4, 37.91% ± 6.70%; GFP DE, n = 7/3, 36.58% ± 4.33%; shNg DE, n = 7/3, 35.78% ± 1.41%, two-way ANOVA, Tukey's multiple comparisons test, *p < 0.05.
(H) Summary bar graph showing % of AMPAR-positive synapses (black) and AMPAR-silent synapses (white) in GFP-AAV- or shNg-AAV-transduced L2/3 pyramidal neurons in V1 in the NR and DE conditions, normalized to the NR condition at P28.

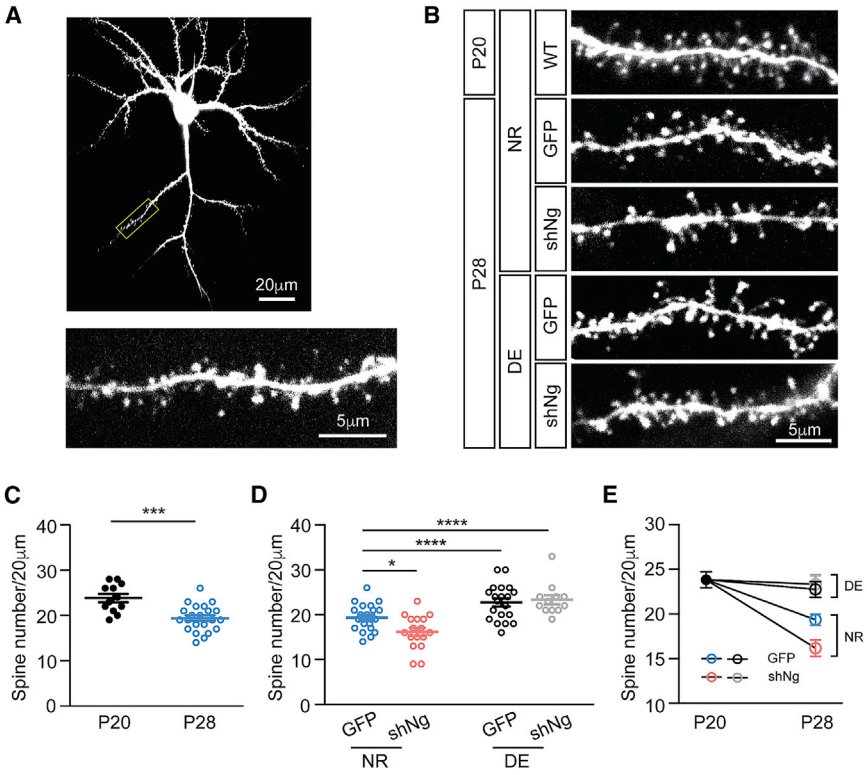

Figure 4. Decrease of Ng Exacerbates Experience-Dependent Decrease of Spine Density

(A) An L2/3 pyramidal neuron filled with Alexa 594 dye in a P28 wild-type mouse. The dendritic segment in the marked box was imaged at high resolution.

(B) Representative images of dendrites from P20 GFP-AAV- and shNg-AAV-transduced neurons at P28 in the NR and DE conditions.

(C) Developmental decrease of spine density from P20 to P28. Summary of spine numbers per 20 μm from P20 (black), n = 12 neurons/3 mice, 23.83 ± 0.90; P28 GFP (open blue), n = 22/4, 19.36 ± 0.66; each data point of PPR is presented with a circle, and mean ± SEM is plotted, Student's t test, ***p < 0.001.

(D) Summary of spine numbers per 20 μm from NR GFP (open blue), NR shNg (open light red), DE GFP (open black), and DE shNg (open gray). GFP NR (replotted from C), n = 22 neurons/4 mice, 19.36 ± 0.66; shNg NR, n = 17/4, 16.18 ± 0.92; GFP DE, n = 22/3, 22.75 ± 0.89; shNg DE, n = 12/4, 23.33 ± 1.03; each data point of PPR is presented with a circle, and mean ± SEM is plotted, two-way ANOVA, Tukey's multiple comparisons test, *p < 0.05, ****p < 0.0001.

(E) Summary of the data, showing further spine loss at P28 caused by decrease of Ng in NR. The data are re-plotted from (C) and (D). Symbols are mean ± SEM.

between Ng and experience influences the excitatory synaptic connectivity.

Ng Regulates Experience-Dependent Spine Elimination during Development

Dendritic spines are the primary postsynaptic site of excitatory synapses in the brain (Yuste and Bonhoeffer, 2004), and both AMPAR-positive and AMPAR-silent synapses have been shown to reside in spines (Béïque et al., 2006). Therefore, spine density can be used as a morphological correlate of the excitatory synaptic connectivity during development and molecular manipulation. To visualize the predicted changes in excitatory synaptic connectivity, we performed spine analysis with our manipulations. We loaded L2/3 pyramidal neurons in visual cortical slices with the fluorescent dye Alexa 594 to measure spine density (Bian et al., 2015). Cell morphology and spine shape were clearly observable in loaded neurons (Figure 4A). We randomly picked the secondary dendrite (~60 μm away from the cell body) of single neurons and analyzed the number of spines in this region. We measured the number of spines from L2/3 pyramidal neurons at two time points during the critical periods of normally reared mice: P20 (untransduced) and P28 (GFP-AAV transduced) (Figures 4B and 4C). P28 mice showed a significantly lower spine density compared to P20 mice (Figures 4B and 4C). The decrease in spine density from P20 to P28 mice was consistent with previous results demonstrating spine elimination during development (Bian et al., 2015).

To test whether Ng affects spine density, we compared shNg-AAV- and GFP-AAV-transduced neurons under the NR and DE conditions (Figures 4B, 4D, and 4E). As expected, shNg-AAV-transduced neurons had a lower spine density compared to GPF-AAV-transduced neurons in NR mice (Figures 4B, 4D, and 4E). The spine density remained high in shNg-AAV- or GFP-AAV-transduced neurons in DE mice (Figures 4B, 4D, and 4E). Thus, decrease of Ng expression accelerated experience-dependent spine elimination. Taken together, our data show that during development, visual experience drives spine elimination from P20 to P28, and loss of Ng leads to the acceleration of this process. Therefore, Ng levels are critical for controlling experience-dependent synapse elimination during this time window.

Decrease of Ng Lowers the Threshold for Induction of Long-Term Depression and Impairs Visually Guided Behavior

Our results so far have revealed that loss of Ng leads to a net loss of both AMPAR-positive and AMPAR-silent synapses and impaired silent synapse maturation, defined by a decrease in the proportion of silent synapses during development (Huang et al., 2015). Given the interaction of Ng and experience in this process, we hypothesized that Ng would regulate the threshold for inducing LTD, a process that depends upon synaptic activity, requires activation of Ca/CaM-dependent phosphatases, and leads to a decrease in AMPAR-mediated transmission and potentially spine elimination (Wiegert and Oertner, 2013). We recorded from GFP-AAV- and shNg-AAV-transduced neurons. We chose to record from DE animals, in which basal synaptic transmission was at similar levels between GFP-AAV- and shNg-AAV-transduced neurons, to avoid the confounding factors of different basal AMPAR- and

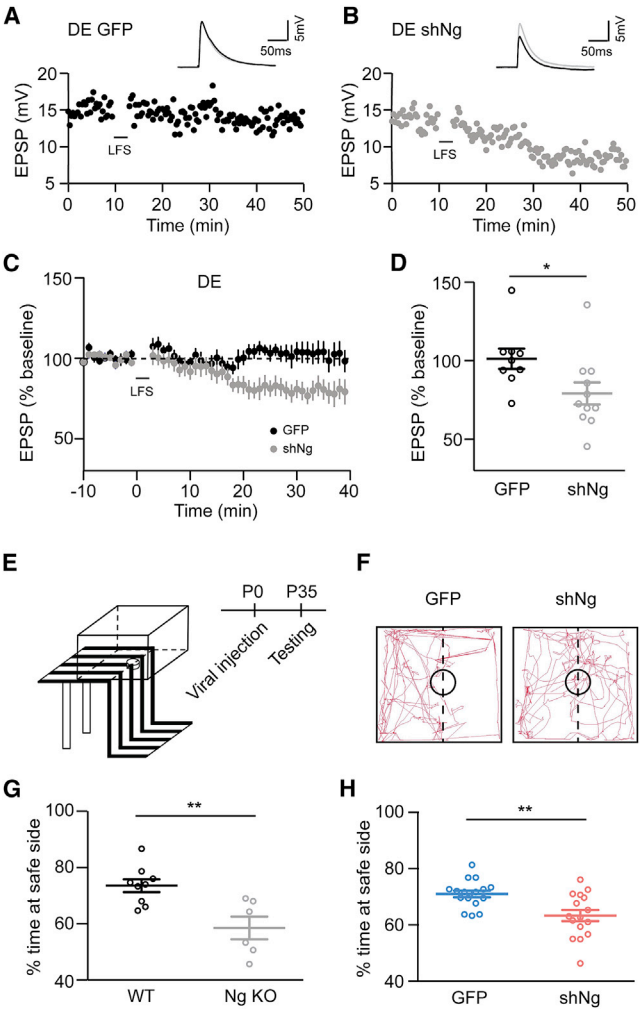

Figure 5. Decrease of Ng Lowered the Threshold for LTD Expression and Impaired Visual Cliff Detection

(A) Representative recording of EPSPs by pairing stimulation from GFP-AAV-transduced neurons in DE. EPSP traces were plotted before (gray) and after (black) pairing stimulation. LFS, low frequency stimulation.

(B) Representative recording of EPSPs by pairing stimulation from shNg-AAV-transduced neurons in DE. EPSP traces were plotted before (gray) and after (black) pairing stimulation.

(C) Time course of % baseline of EPSPs recorded at L4–L2/3 synapses from GFP-AAV- (black) and shNg-AAV- (gray) transduced neurons in DE.

(D) Percentage of baseline EPSP amplitude of averaged EPSP amplitude recorded from 30 to 40 min in GFP-AAV- and shNg-AAV-transduced neurons. GFP, n = 9 slices/5 mice, 101.28% ± 6.47%; shNg, n = 11/7, 79.18% ± 7.08%; each data point of PPR is presented with a circle, and mean ± SEM is plotted, Student's t test, *$p < 0.05$.

(E) The visual cliff apparatus and timeline for viral injection.

(F) Example plots of tracking of mouse movement for 5 min of GFP-AAV- and shNg-AAV-transduced mice, tested at P35.

(G) Percentage of time stayed at safe side for WT littermates (open black) and Ng KO (open gray) mice. WT, n = 9 mice, 73.56% ± 2.27%; Ng KO, n = 6 mice, 58.5% ± 4.03%; each data point of PPR is presented with a circle, and mean ± SEM is plotted, Student's t test, **$p < 0.01$.

(H) Percentage of time stayed at safe side for GFP-AAV (open blue) and shNg-AAV-transduced (open light red) mice. GFP, n = 14 mice, 71.38% ± 1.12%; shNg, n = 15, 63.35% ± 1.96%; each data point of PPR is presented with a circle, and mean ± SEM is plotted, Student's t test, **$p < 0.01$.

NMDAR-mediated transmission (Figure 3). Using a pairing protocol that did not induce LTD at L4–L2/3 synapses in L2/3 GFP-AAV-transduced pyramidal neurons (Choi et al., 2005), we were able to elicit reliable LTD in shNg-AAV-transduced neurons (Figures 5A–5D), suggesting that decreased Ng renders L4–L2/3 synapses more vulnerable to LTD. This observation offers a plausible explanation as to why visual experience leads to exacerbated elimination of synapses when Ng is reduced.

To further test the effect of a decrease of Ng on visual system function, we performed the visual cliff test to test visual perception-guided behavior (Figure 5E) (Lione et al., 1999; Walk et al., 1957) at P35, once V1 had reached functional maturity (Espinosa and Stryker, 2012). The mice were placed in the center of an arena with a transparent floor extending outside of the edge of the table top, revealing an apparent cliff (Figure 5E). The whiskers were trimmed before the task to minimize somatosensory input from active whisking. If mice can visually discriminate a drop at the edge of the cliff, they will prefer to explore the safe side (the bench top). The behavioral performance of mice was measured by the percentage of time they spent on the safe side of the arena (Figure 5F). We tested the Ng KO mice in comparison to their WT littermates. WT mice showed a clear preference for the safe side of the arena, suggesting they can visually distinguish the cliff, whereas the Ng KO mice showed a deficit in this task (Figure 5G). To test whether the deficit depends on the primary visual cortex, we injected shNg-AAV and GFP-AAV into the visual cortex at P0 to specifically knock down Ng only in V1. Similar to the Ng KO mice, shNg-AAV-transduced animals also showed a deficit in this task in comparison to the GFP-AAV-injected mice (Figure 5H), suggesting that the decrease in Ng levels in V1 impaired visual perception in the mice.

Taken together, our results demonstrate that visual experience leads to an equilibrium of AMPAR-positive synapses and a net loss of AMPAR-silent synapses in L2/3 principal neurons in V1 during the critical period of visual cortical development. This equilibrium is most likely due to the coordinated conversion of AMPAR-silent synapses to AMPAR-positive synapses and experience-dependent pruning of excitatory glutamatergic synapses. The overall change in synapse number is also reflected in the decrease in spine numbers. These data imply that Ng coordinates the processes of experience-dependent AMPAR-silent synapse maturation and synapse elimination. When Ng levels are decreased, synapses become vulnerable, leading to accelerated spine elimination, potentially via sensitized LTD, and halting of AMPAR-silent synapse maturation. Consequently, loss of Ng leads to impaired synaptic plasticity and impaired visually guided behavior. These results therefore indicate that Ng acts as an essential coordinator for balanced and constructive synaptic refinement during visual cortical postnatal development.

DISCUSSION

Neural activity resulting from sensory experience is required for the refinement and maturation of neural circuits during cortical critical periods. This refinement is thought to be important for functional optimization of primary sensory cortices, enabling critical functions such as feature detection (Kang et al., 2013; Wang

et al., 2013). Here we show that AMPAR-positive synapses are maintained at an equilibrium in V1, accompanied by a net loss of AMPAR-silent synapses during the critical period of cortical plasticity, resulting in a decrease in total glutamatergic synapse numbers. We demonstrate that Ng coordinates balanced, experience-driven AMPAR-silent synapse conversion and glutamatergic synapse elimination in L2/3 pyramidal neurons in V1 to achieve functional maturation and optimization of the cortical excitatory circuitry.

Our results support the notion that AMPAR-positive synapses are reorganized during the critical period leading to excitatory circuit maturation. This circuit maturation is likely mediated by the combined effect of AMPAR-silent synapse maturation, defined by decreasing the proportion of silent synapses and increasing the AMPAR/NMDAR EPSC ratio (Huang et al., 2015) and the elimination of existing glutamatergic synapses (Bian et al., 2015; Holtmaat et al., 2005; Zuo et al., 2005a). These two processes are coordinated to maintain the equilibrium of AMPAR-positive synapses. It is noteworthy that conversion of AMPAR-silent synapses to AMPAR-positive synapses likely contributes to this progressive AMPAR-silent synapse maturation (Ashby and Isaac, 2011; Huang et al., 2015; Wu et al., 1996), which should lead to an overall enhancement of AMPAR-mediated synaptic transmission. However, the equilibrium in AMPAR-mediated synaptic transmission implies that some existing AMPAR-positive synapses must go through experience-dependent downregulation and counteract the AMPAR-silent synapse conversion for excitatory circuit maturation. The finding of a net loss of total synapses and AMPAR-silent synapses is in agreement with previous morphological studies showing a net decrease in spine density during development, preferentially in thin spines, which are thought to represent immature, weaker, or AMPAR-silent synapses (Bian et al., 2015; Holtmaat et al., 2005; Zuo et al., 2005a). Although our data do not provide direct evidence for the life cycle of glutamatergic synapses, based upon our functional analyses it is likely that both AMPAR-positive and AMPAR-silent synapses are eliminated during the critical period. Interestingly, experience-dependent re-silencing of AMPAR-positive synapses has been shown in the nucleus accumbens under special circumstances (Graziane et al., 2016), providing an intriguing possibility for AMPAR-positive synapse elimination. Further experiments are required to differentiate these possibilities and measure the dynamics of AMPAR-silent synapse maturation and synapse elimination. Importantly, our results imply that AMPAR-silent synapse maturation is part of the excitatory circuit maturation process via coordinated spine elimination and AMPAR-silent synapse conversion during heightened experience-dependent cortical plasticity.

Consistent with previous reports, our results indicate that sensory deprivation prevents AMPAR-silent synapse maturation (Funahashi et al., 2013). Our results further show that sensory deprivation arrests synapses at the early developmental stage, with a higher proportion of AMPAR-silent synapses and a sustained number of AMPAR-positive synapses. It is likely that both experience-dependent synapse elimination and AMPAR-silent synapse conversion are prevented by sensory deprivation.

Remarkably, the function of the CaM-complexing protein Ng is essential for this experience-dependent coordination. Loss of Ng broke the experience-dependent equilibrium of AMPAR-positive synapses, induced the loss of AMPAR-positive synapses, and halted AMPAR-silent synapse maturation. Deprivation of sensory input to V1 prevented the deterioration in synaptic transmission caused by loss of Ng and likely arrested the circuit at an earlier developmental stage prior to sensory deprivation (Figures 1 and 3). These results highlight the critical involvement of Ng in coordinating experience-dependent refinement of cortical excitatory circuitry.

We found that decreased Ng levels lead to a lower threshold for LTD induction at L4–L2/3 synapses. Previous studies in hippocampal slice culture have shown that LTD at individual synapses induces spine elimination at both the targeted synapse and selective neighboring synapses when spines are monitored a few days following stimulation (Wiegert and Oertner, 2013). It is therefore conceivable that visual input triggers spine elimination in L2/3 pyramidal neurons in V1 using the cellular mechanism of LTD, and that a decrease in Ng enhances this vulnerability by lowering the threshold for LTD. Given the high proportion of AMPAR-silent synapses after reduction of Ng, it is likely that the conversion of AMPAR-silent synapses to AMPAR-positive synapses is also impaired. Our results support the hypothesis that Ng levels in L2/3 pyramidal neurons control the Ca^{2+}/CaM-dependent signaling sensitivity and orchestrate experience-dependent AMPAR-silent synapse conversion and synapse elimination.

It is noteworthy that dysfunction of Ca^{2+} homeostasis is involved in many neurological and neuropsychiatric diseases (Bojarski et al., 2010; Chan et al., 2009; Green and LaFerla, 2008). Genome-wide association studies have identified Ng as a candidate gene close to a risk-carrying allele (Stefansson et al., 2009), and Ng levels are significantly reduced in the prefrontal cortex of schizophrenia patients (Broadbelt et al., 2006). Interestingly, recent genetic evidence highlighted the complement component 4 (C4) genes, suggesting a potential role of heightened synapse elimination during postnatal development in schizophrenia (Sekar et al., 2016). Dendritic spine loss is also observed in neurodegenerative diseases including Alzheimer's disease and Huntington's disease (Fiala et al., 2002; Spires et al., 2004). It has been shown that overexpression of Ng restores synaptic transmission and LTP, both of which are impaired by amyloid V application (Kaleka and Gerges, 2016). Our results thus provide a potential clue to the pathophysiology underlying aberrant neural circuit refinement in neuropsychiatric and neurodegenerative disorders associated with aberrant Ca^{2+}-dependent signaling.

In conclusion, our studies offer insight into how Ng regulates experience-dependent cortical excitatory circuit optimization. Our analyses reconcile the functional and anatomical observations in experience-dependent developmental modification of glutamatergic cortical synapses and provide a general mechanism concerning experience-dependent dynamic reorganization of glutamatergic synaptic transmission: progressive elimination of glutamatergic synapses upon experience and conversion of AMPAR-silent synapses to AMPAR-positive synapses together maintain AMPAR-positive synapses at equilibrium during the

critical period to achieve cortical excitatory circuit maturation. Decreased Ng expression breaks the balance of these processes and leads to a loss of AMPAR-positive synapses and delayed AMPAR-silent synapse maturation. We propose that sensory experience coordinates these two experience-dependent cellular processes through Ng-dependent regulation of Ca^{2+}/CaM-dependent signaling pathways to functionally optimize neural circuits.

EXPERIMENTAL PROCEDURES

Animals

Male neurogranin knockout (Jackson Laboratory) and C57BL/6 mice (Charles River) were used for all electrophysiological and behavioral experiments. All animals were maintained in a vivarium with a light/dark cycle (7:00 a.m.∼7:00 p.m.). Animal care and handling were performed according to NIH guidelines and with the approval of the Massachusetts Institute of Technology (MIT) institutional animal care and use committee (IACUC) and Division of Comparative Medicine (DCM).

Viral Production

AAV1/2 was produced in HEK-T cells (ATCC) as previously described (Grieger et al., 2006). Cells were transfected with an AAV expression vector and corresponding helper plasmids. Sixty to 72 hr posttransfection, the virus was purified using discontinuous iodixanol gradients. Virus titers were tested with either the qPCR amplification of genomic copy number or the serial dilution infection of primary neuronal culture.

Viral Injection

Male C57BL/6 mice were prepared for surgery using standard procedures in accordance with NIH guidelines and with the approval of the MIT IACUC and DCM. Animals were anesthetized with a mixture of Ketamine (100mg/kg body weight) and xylazine (10mg/kg body weight) and subsequently immobilized on a stereotactic apparatus (Harvard Apparatus). The coordinates for the primary visual cortex are anterior-posterior (AP), −3.5 mm; medial-lateral (ML), ±2.5 mm from bregma; dorsal-ventral (DV), −0.3∼0.5 mm below the dura; 0.5 μL of virus was injected using a nanoinjector (Harvard Apparatus). The scalp was sutured and Buprenex analgesic (0.1 mg/kg) was given subcutaneously in accordance with the guidelines.

Western Blot

Mice were injected with GFP-AAV, shLc-AAV, and shNg-AAV in the primary visual cortex. A detailed sample preparation procedure is in Supplemental Experimental Procedures. Primary antibodies were anti-neurogranin (Millipore; AB5620), 1:3,000; anti-actin (Sigma; A2228), 1:5,000; anti-CaMKIIα (Epitomics; 2716-1), 1:2,000; and anti-CaM (Millipore; 05-173), 1:1,000. Signals from infrared secondary antibodies (goat anti-mouse 700 and goat anti-rabbit 800; LI-COR; 1:5,000) were detected on an Odyssey scanner (LI-COR), and band intensities were quantified using ImageJ (NIH).

Visual Cortical Slice Electrophysiology

Mice were deeply anesthetized with isoflurane and decapitated following disappearance of the righting reflex. The brain was rapidly removed and submerged in an ice-cold choline-based dissection buffer bubbled with 95% O_2/5% CO_2 mixture. Coronal slices (300–350 μm) from the visual cortex were prepared using an HM 650V vibratome (Thermo Scientific). The slices were collected in ice-cold dissection buffer and gently transferred to an incubation chamber with artificial cerebrospinal fluid (ACSF) saturated with 95% O_2/5% CO_2. The slices recovered at room temperature for 1 hr before recording.

Visual cortical slices were transferred to the recording chamber, maintained at 29°C, and constantly perfused with ACSF saturated with 95% O_2/5% CO_2. L2/3 neurons were visually identified with infrared differential interference contrast optics on an Olympus BX51WI upright microscope. Recordings were done by standard procedures. Detailed experimental procedures are in Supplemental Experimental Procedures. Neurons were recorded in a whole-cell patch-clamp configuration with a MultiClamp 700B amplifier (Axon Instruments), and data were filtered at 2 kHz and digitized at 10 kHz using Igor Pro (WaveMetrics).

For procedures for miniature EPSC recordings, AMPAR/NMDAR ratio, and minimum stimulation for failure analyses, see Supplemental Experimental Procedures. To calculate the relative proportion of AMPAR-transmitting and AMPAR-silent synapses, all experimental conditions were normalized to the control condition in P28 mice. Averaged mEPSC frequencies were used to calculate the proportion of AMPAR-transmitting synapses relative to the control condition. The relative proportion of AMPAR-silent synapses was then scaled accordingly using the data from the failure analyses.

Fluorescent Dye Microinjection

Fluorescent dye injection was carried out as previously described (Bian et al., 2015). Detailed experimental procedures are in Supplemental Experimental Procedures.

Visual Cliff Discrimination

The experiment was conducted in an open-top Perspex box measuring 40 cm × 40 cm × 30 cm, which was placed on the edge of a laboratory bench so that half of the box was on the bench (safe side) and the other half was 80 cm above the floor (cliff side). A black-and-white-striped pattern was placed under the box and on the floor on the cliff side to emphasize the cliff dropoff. The main light source was dimmed. A circular Perspex platform (9-cm diameter × 1.5 cm) was placed in the center of the box to allow the mouse to view its surroundings. Each mouse was placed on the platform and observed for 5 min beginning from its placement on the platform. Each mouse received a single trial. We trimmed the whiskers of the animals 1 hr before each trial to ensure the engagement of the visual sensory system. The box and platform were cleaned with quatricide and 70% alcohol after each trial.

Statistical Analysis

Statistical analysis was performed using Prism (GraphPad). Data are presented as mean ± SEM. Two-sample t test was used for comparison of two groups of data after normality test. With more than two groups of data with single-factor manipulation, differences were determined using one-way ANOVA with Tukey's post hoc test unless otherwise noted. Two-factor datasets were analyzed using two-way ANOVA with Tukey's post hoc test. p values of <0.05 were considered significant.

SUPPLEMENTAL INFORMATION

Supplemental Information includes Supplemental Experimental Procedures and five figures and can be found with this article online at http://dx.doi.org/10.1016/j.celrep.2016.12.084.

AUTHOR CONTRIBUTIONS

Conceptualization, K.-S.H. and W.X.; Methodology, K.-S.H., S.F.C., and W.X.; Investigation, K.-S.H. and S.F.C.; Writing – Original Draft, K.-S.H. and W.X.; Writing – Review & Editing, K.-S.H., S.F.C., and W.X.; Funding Acquisition, K.-S.H. and W.X.; Supervision, W.X.

ACKNOWLEDGMENTS

This work was supported by the JPB Foundation, Whitehall Foundation, and Broad Institute Stanley Center. We thank Drs. Mark F. Bear, Elly Nedivi, Oliver M. Schluter, Steven Flavell, Martha Constantine-Paton, Jianhua Cang, and members of the W.X. laboratory for their helpful comments, Drs. Wen-Jie Bian and Xiang Yu for their help with spine imaging, and Cynthia Hou, Emily Liao, Xiaobai Ren, and Taekeun Kim for their excellent technical support.

Received: July 1, 2016
Revised: November 21, 2016
Accepted: December 26, 2016
Published: January 24, 2017

REFERENCES

Antonini, A., and Stryker, M.P. (1993). Rapid remodeling of axonal arbors in the visual cortex. Science *260*, 1819–1821.

Ashby, M.C., and Isaac, J.T. (2011). Maturation of a recurrent excitatory neocortical circuit by experience-dependent unsilencing of newly formed dendritic spines. Neuron *70*, 510–521.

Baimbridge, K.G., Celio, M.R., and Rogers, J.H. (1992). Calcium-binding proteins in the nervous system. Trends Neurosci. *15*, 303–308.

Becker, N., Wierenga, C.J., Fonseca, R., Bonhoeffer, T., and Nägerl, U.V. (2008). LTD induction causes morphological changes of presynaptic boutons and reduces their contacts with spines. Neuron *60*, 590–597.

Béïque, J.C., Lin, D.T., Kang, M.G., Aizawa, H., Takamiya, K., and Huganir, R.L. (2006). Synapse-specific regulation of AMPA receptor function by PSD-95. Proc. Natl. Acad. Sci. USA *103*, 19535–19540.

Bian, W.J., Miao, W.Y., He, S.J., Qiu, Z., and Yu, X. (2015). Coordinated spine pruning and maturation mediated by inter-spine competition for cadherin/catenin complexes. Cell *162*, 808–822.

Bojarski, L., Debowska, K., and Wojda, U. (2010). In vitro findings of alterations in intracellular calcium homeostasis in schizophrenia. Prog. Neuropsychopharmacol. Biol. Psychiatry *34*, 1367–1374.

Broadbelt, K., Ramprasaud, A., and Jones, L.B. (2006). Evidence of altered neurogranin immunoreactivity in areas 9 and 32 of schizophrenic prefrontal cortex. Schizophr. Res. *87*, 6–14.

Chan, C.S., Gertler, T.S., and Surmeier, D.J. (2009). Calcium homeostasis, selective vulnerability and Parkinson's disease. Trends Neurosci. *32*, 249–256.

Choi, S.Y., Chang, J., Jiang, B., Seol, G.H., Min, S.S., Han, J.S., Shin, H.S., Gallagher, M., and Kirkwood, A. (2005). Multiple receptors coupled to phospholipase C gate long-term depression in visual cortex. J. Neurosci. *25*, 11433–11443.

Coldren, C.D., Lai, Z., Shragg, P., Rossi, E., Glidewell, S.C., Zuffardi, O., Mattina, T., Ivy, D.D., Curfs, L.M., Mattson, S.N., et al. (2009). Chromosomal microarray mapping suggests a role for BSX and neurogranin in neurocognitive and behavioral defects in the 11q terminal deletion disorder (Jacobsen syndrome). Neurogenetics *10*, 89–95.

Espinosa, J.S., and Stryker, M.P. (2012). Development and plasticity of the primary visual cortex. Neuron *75*, 230–249.

Fagiolini, M., Pizzorusso, T., Berardi, N., Domenici, L., and Maffei, L. (1994). Functional postnatal development of the rat primary visual cortex and the role of visual experience: dark rearing and monocular deprivation. Vision Res. *34*, 709–720.

Fiala, J.C., Spacek, J., and Harris, K.M. (2002). Dendritic spine pathology: cause or consequence of neurological disorders? Brain Res. Brain Res. Rev. *39*, 29–54.

Funahashi, R., Maruyama, T., Yoshimura, Y., and Komatsu, Y. (2013). Silent synapses persist into adulthood in layer 2/3 pyramidal neurons of visual cortex in dark-reared mice. J. Neurophysiol. *109*, 2064–2076.

Gaertner, T.R., Putkey, J.A., and Waxham, M.N. (2004). RC3/neurogranin and Ca^{2+}/calmodulin-dependent protein kinase II produce opposing effects on the affinity of calmodulin for calcium. J. Biol. Chem. *279*, 39374–39382.

Glazewski, S., Chen, C.M., Silva, A., and Fox, K. (1996). Requirement for alpha-CaMKII in experience-dependent plasticity of the barrel cortex. Science *272*, 421–423.

Graziane, N.M., Sun, S., Wright, W.J., Jang, D., Liu, Z., Huang, Y.H., Nestler, E.J., Wang, Y.T., Schlüter, O.M., and Dong, Y. (2016). Opposing mechanisms mediate morphine- and cocaine-induced generation of silent synapses. Nat. Neurosci. *19*, 915–925.

Green, K.N., and LaFerla, F.M. (2008). Linking calcium to Abeta and Alzheimer's disease. Neuron *59*, 190–194.

Grieger, J.C., Choi, V.W., and Samulski, R.J. (2006). Production and characterization of adeno-associated viral vectors. Nat. Protoc. *1*, 1412–1428.

Higo, N., Oishi, T., Yamashita, A., Matsuda, K., and Hayashi, M. (2004). Cell type- and region-specific expression of neurogranin mRNA in the cerebral cortex of the macaque monkey. Cereb. Cortex *14*, 1134–1143.

Holtmaat, A.J., Trachtenberg, J.T., Wilbrecht, L., Shepherd, G.M., Zhang, X., Knott, G.W., and Svoboda, K. (2005). Transient and persistent dendritic spines in the neocortex in vivo. Neuron *45*, 279–291.

Huang, K.P., Huang, F.L., Jäger, T., Li, J., Reymann, K.G., and Balschun, D. (2004). Neurogranin/RC3 enhances long-term potentiation and learning by promoting calcium-mediated signaling. J. Neurosci. *24*, 10660–10669.

Huang, X., Stodieck, S.K., Goetze, B., Cui, L., Wong, M.H., Wenzel, C., Hosang, L., Dong, Y., Löwel, S., and Schlüter, O.M. (2015). Progressive maturation of silent synapses governs the duration of a critical period. Proc. Natl. Acad. Sci. USA *112*, E3131–E3140.

Isaac, J.T., Nicoll, R.A., and Malenka, R.C. (1995). Evidence for silent synapses: implications for the expression of LTP. Neuron *15*, 427–434.

Ishikawa, A.W., Komatsu, Y., and Yoshimura, Y. (2014). Experience-dependent emergence of fine-scale networks in visual cortex. J. Neurosci. *34*, 12576–12586.

Kaleka, K.S., and Gerges, N.Z. (2016). Neurogranin restores amyloid β-mediated synaptic transmission and long-term potentiation deficits. Exp. Neurol. *277*, 115–123.

Kang, E., Durand, S., LeBlanc, J.J., Hensch, T.K., Chen, C., and Fagiolini, M. (2013). Visual acuity development and plasticity in the absence of sensory experience. J. Neurosci. *33*, 17789–17796.

Kirkwood, A., Lee, H.K., and Bear, M.F. (1995). Co-regulation of long-term potentiation and experience-dependent synaptic plasticity in visual cortex by age and experience. Nature *375*, 328–331.

Liao, D., Hessler, N.A., and Malinow, R. (1995). Activation of postsynaptically silent synapses during pairing-induced LTP in CA1 region of hippocampal slice. Nature *375*, 400–404.

Lione, L.A., Carter, R.J., Hunt, M.J., Bates, G.P., Morton, A.J., and Dunnett, S.B. (1999). Selective discrimination learning impairments in mice expressing the human Huntington's disease mutation. J. Neurosci. *19*, 10428–10437.

Malinow, R., Madison, D.V., and Tsien, R.W. (1988). Persistent protein kinase activity underlying long-term potentiation. Nature *335*, 820–824.

Meyer, T., Hanson, P.I., Stryer, L., and Schulman, H. (1992). Calmodulin trapping by calcium-calmodulin-dependent protein kinase. Science *256*, 1199–1202.

Mulkey, R.M., Endo, S., Shenolikar, S., and Malenka, R.C. (1994). Involvement of a calcineurin/inhibitor-1 phosphatase cascade in hippocampal long-term depression. Nature *369*, 486–488.

Pak, J.H., Huang, F.L., Li, J., Balschun, D., Reymann, K.G., Chiang, C., Westphal, H., and Huang, K.P. (2000). Involvement of neurogranin in the modulation of calcium/calmodulin-dependent protein kinase II, synaptic plasticity, and spatial learning: a study with knockout mice. Proc. Natl. Acad. Sci. USA *97*, 11232–11237.

Petersen, A., and Gerges, N.Z. (2015). Neurogranin regulates CaM dynamics at dendritic spines. Sci. Rep. *5*, 11135.

Phillips, M.A., Colonnese, M.T., Goldberg, J., Lewis, L.D., Brown, E.N., and Constantine-Paton, M. (2011). A synaptic strategy for consolidation of convergent visuotopic maps. Neuron *71*, 710–724.

Represa, A., Deloulme, J.C., Sensenbrenner, M., Ben-Ari, Y., and Baudier, J. (1990). Neurogranin: immunocytochemical localization of a brain-specific protein kinase C substrate. J. Neurosci. *10*, 3782–3792.

Ruano, D., Aulchenko, Y.S., Macedo, A., Soares, M.J., Valente, J., Azevedo, M.H., Hutz, M.H., Gama, C.S., Lobato, M.I., Belmonte-de-Abreu, P., et al. (2008). Association of the gene encoding neurogranin with schizophrenia in males. J. Psychiatr. Res. *42*, 125–133.

Rumpel, S., Hatt, H., and Gottmann, K. (1998). Silent synapses in the developing rat visual cortex: evidence for postsynaptic expression of synaptic plasticity. J. Neurosci. *18*, 8863–8874.

Sekar, A., Bialas, A.R., de Rivera, H., Davis, A., Hammond, T.R., Kamitaki, N., Tooley, K., Presumey, J., Baum, M., Van Doren, V., et al.; Schizophrenia Working Group of the Psychiatric Genomics Consortium (2016). Schizophrenia risk from complex variation of complement component 4. Nature *530*, 177–183.

Silva, A.J., Wang, Y., Paylor, R., Wehner, J.M., Stevens, C.F., and Tonegawa, S. (1992). Alpha calcium/calmodulin kinase II mutant mice: deficient long-term potentiation and impaired spatial learning. Cold Spring Harb. Symp. Quant. Biol. *57*, 527–539.

Singec, I., Knoth, R., Ditter, M., Volk, B., and Frotscher, M. (2004). Neurogranin is expressed by principal cells but not interneurons in the rodent and monkey neocortex and hippocampus. J. Comp. Neurol. *479*, 30–42.

Slemmon, J.R., Feng, B., and Erhardt, J.A. (2000). Small proteins that modulate calmodulin-dependent signal transduction: effects of PEP-19, neuromodulin, and neurogranin on enzyme activation and cellular homeostasis. Mol. Neurobiol. *22*, 99–113.

Spires, T.L., Grote, H.E., Garry, S., Cordery, P.M., Van Dellen, A., Blakemore, C., and Hannan, A.J. (2004). Dendritic spine pathology and deficits in experience-dependent dendritic plasticity in R6/1 Huntington's disease transgenic mice. Eur. J. Neurosci. *19*, 2799–2807.

Stefansson, H., Ophoff, R.A., Steinberg, S., Andreassen, O.A., Cichon, S., Rujescu, D., Werge, T., Pietiläinen, O.P., Mors, O., Mortensen, P.B., et al.; Genetic Risk and Outcome in Psychosis (GROUP) (2009). Common variants conferring risk of schizophrenia. Nature *460*, 744–747.

Taha, S., Hanover, J.L., Silva, A.J., and Stryker, M.P. (2002). Autophosphorylation of alphaCaMKII is required for ocular dominance plasticity. Neuron *36*, 483–491.

Torii, N., Kamishita, T., Otsu, Y., and Tsumoto, T. (1995). An inhibitor for calcineurin, FK506, blocks induction of long-term depression in rat visual cortex. Neurosci. Lett. *185*, 1–4.

Walk, R.D., Gibson, E.J., and Tighe, T.J. (1957). Behavior of light- and dark-reared rats on a visual cliff. Science *126*, 80–81.

Wang, B.S., Feng, L., Liu, M., Liu, X., and Cang, J. (2013). Environmental enrichment rescues binocular matching of orientation preference in mice that have a precocious critical period. Neuron *80*, 198–209.

Watson, J.B., Sutcliffe, J.G., and Fisher, R.S. (1992). Localization of the protein kinase C phosphorylation/calmodulin-binding substrate RC3 in dendritic spines of neostriatal neurons. Proc. Natl. Acad. Sci. USA *89*, 8581–8585.

Wiegert, J.S., and Oertner, T.G. (2013). Long-term depression triggers the selective elimination of weakly integrated synapses. Proc. Natl. Acad. Sci. USA *110*, E4510–E4519.

Wu, G., Malinow, R., and Cline, H.T. (1996). Maturation of a central glutamatergic synapse. Science *274*, 972–976.

Yuste, R., and Bonhoeffer, T. (2004). Genesis of dendritic spines: insights from ultrastructural and imaging studies. Nat. Rev. Neurosci. *5*, 24–34.

Zeng, H., Chattarji, S., Barbarosie, M., Rondi-Reig, L., Philpot, B.D., Miyakawa, T., Bear, M.F., and Tonegawa, S. (2001). Forebrain-specific calcineurin knockout selectively impairs bidirectional synaptic plasticity and working/episodic-like memory. Cell *107*, 617–629.

Zhabotinsky, A.M., Camp, R.N., Epstein, I.R., and Lisman, J.E. (2006). Role of the neurogranin concentrated in spines in the induction of long-term potentiation. J. Neurosci. *26*, 7337–7347.

Zhong, L., Brown, J., Kramer, A., Kaleka, K., Petersen, A., Krueger, J.N., Florence, M., Muelbl, M.J., Battle, M., Murphy, G.G., et al. (2015). Increased prefrontal cortex neurogranin enhances plasticity and extinction learning. J. Neurosci. *35*, 7503–7508.

Zhou, Q., Homma, K.J., and Poo, M.M. (2004). Shrinkage of dendritic spines associated with long-term depression of hippocampal synapses. Neuron *44*, 749–757.

Zuo, Y., Lin, A., Chang, P., and Gan, W.B. (2005a). Development of long-term dendritic spine stability in diverse regions of cerebral cortex. Neuron *46*, 181–189.

Zuo, Y., Yang, G., Kwon, E., and Gan, W.B. (2005b). Long-term sensory deprivation prevents dendritic spine loss in primary somatosensory cortex. Nature *436*, 261–265.